miR-218 regulates focal adhesion kinase–dependent TGFβ signaling in fibroblasts

Fen Guo[a], David E. Carter[b], and Andrew Leask[a,c]
[a]Department of Dentistry and [c]Department of Physiology and Pharmacology, University of Western Ontario, London, ON N6A 5C1, Canada; [b]London Regional Genomics Centre Microarray Facility, Robarts Research Institute, London, ON N6A 5K8, Canada

ABSTRACT Scarring, which occurs in essentially all adult tissue, is characterized by the excessive production and remodeling of extracellular matrix by α-smooth muscle actin (SMA)–expressing myofibroblasts located within connective tissue. Excessive scarring can cause organ failure and death. Oral gingivae do not scar. Compared to dermal fibroblasts, gingival fibroblasts are less responsive to transforming growth factor β (TGFβ) due to the reduced expression, due to the reduced expression and activity of focal adhesion kinase (FAK) by this cell type. Here we show that, compared with dermal fibroblasts, gingival fibroblasts show reduced expression of miR-218. Introduction of pre–miR-218 into gingival fibroblasts elevates FAK expression and, via a FAK/src-dependent mechanism, results in the ability of TGFβ to induce α-SMA. The deubiquitinase cezanne is a direct target of miR-218 and has increased expression in gingival fibroblasts compared with dermal fibroblasts. Knockdown of cezanne in gingival fibroblasts increases FAK expression and causes TGFβ to induce α-smooth muscle actin (α-SMA). These results suggest that miR-218 regulates the ability of TGFβ to induce myofibroblast differentiation in fibroblasts via cezanne/FAK.

INTRODUCTION

In adult humans, scarring is a normal response to tissue injury. Excessive deposition of scar tissue can cause fibrotic diseases, which are characterized by progressive tissue damage often resulting in organ failure and death. Collectively these diseases represent one of the largest groups of disease for which there is no treatment (Wynn and Ramalingam, 2012). Scarring, a natural response to wounding in adult tissue, including skin, does not occur in the oral cavity (Schor et al., 1996). Instead of a fibrocontractile response characterized by the presence of abundant α-smooth muscle actin (SMA)–containing myofibroblasts, the fibrotic response in oral tissue

is principally fibroproliferative and is largely devoid of myofibroblasts (Sakamoto et al., 2002; Martelli et al., 2010; Damasceno et al., 2012). Understanding why gingiva and skin behave differently in response to fibrotic stimuli should yield valuable insights into how to achieve scarless repair.

Connective tissue is largely composed of extracellular matrix (ECM) and fibroblasts (Canady et al., 2013). Fibroblasts display distinct gene patterns based on their location in the body; accordingly, it is reasonable to hypothesize that fibroblasts at different locations in the body are, in fact, distinct differentiated cell types (Chang et al., 2002). Thus differential responses of gingival versus dermal fibroblasts to fibrogenic stimuli could underlie scarless tissue repair. Consistent with this idea, we showed that compared with dermal fibroblasts, gingival fibroblasts are less responsive to mechanical strain and to the potent fibrogenic cytokine transforming growth factor β (TGFβ; Guo et al., 2011a). TGFβ potently induces myofibroblast differentiation, as observed by α-SMA mRNA and protein expression, in dermal but not gingival fibroblasts (Ghosh et al., 2004; Shephard et al., 2004b; Guo et al., 2011a). TGFβ signals through cell adhesion via src/focal adhesion kinase (FAK) to promote collagen production and myofibroblast differentiation (Thannickal et al., 2003; Mishra et al., 2007; Liu et al., 2007). Compared to dermal fibroblasts, gingival fibroblasts express less FAK and are less adhesive to ECM (Guo et al., 2011b). This difference in adhesive capacity appears to underlie the

differential responses of dermal and gingival fibroblasts to TGFβ (Guo et al., 2011a,b). However, the molecular basis for the reduced expression of FAK and hence for the relative inability of TGFβ to induce α-SMA expression in gingival fibroblasts is unclear.

MicroRNAs (miRNAs)—small, noncoding RNAs that act to modulate posttranscriptional and transcriptional gene regulation—are well conserved in evolution and are believed to represent an ancient component of gene regulation. Several different miRNAs have been shown to be dysregulated in fibrotic conditions (Mann and Mann, 2013), and thus it is possible that alterations in miRNA expression patterns may underlie the phenotypic differences between gingival and dermal fibroblasts. In this article, we evaluate this hypothesis. Our results therefore suggest a basis for the relative inability of TGFβ to induce myofibroblast differentiation in gingival fibroblasts and hence offer potential insight into the basis of scarless tissue repair.

RESULTS

miR-218 shows reduced expression in human gingival fibroblasts

Previously we found that gingival fibroblasts are relatively less responsive to TGFβ than are dermal fibroblasts (Guo et al., 2011a). In particular, the ability of TGFβ to induce α-SMA protein and mRNA in gingival fibroblasts is severely impaired compared with dermal
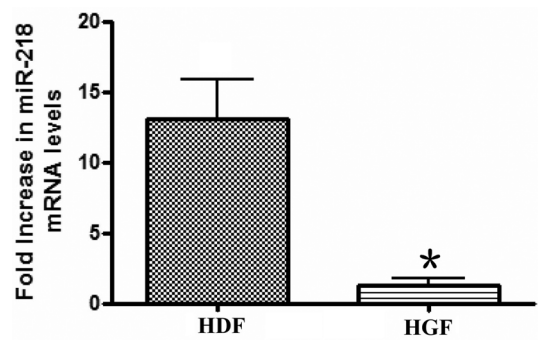

FIGURE 1: Expression levels of miR-218 are higher in human dermal fibroblasts than in human gingival fibroblasts. As described in *Materials and Methods*, RNA was prepared from human dermal fibroblasts (HDFs) and human gingival fibroblasts (HGFs) and subjected to real-time PCR analysis to detect miR-218. Relative expression compared with HGFs ($N = 3$, $*p < 0.05$, Student's t test).

fibroblasts (Guo et al., 2011a); the differential ability of TGFβ to signal in gingival fibroblasts was attributed to reduced FAK expression and FAK/src-dependent signaling in this cell type (Guo et al., 2011a,b). To begin to identify miRNAs that might be responsible for this difference, we conducted microarray analysis of RNAs prepared from dermal and gingival fibroblasts. We identified 24 miRNAs that were increased in dermal fibroblasts (Table 1). Of these, miR-218 was selected for further analysis, as this miRNA is activated by src (Li et al., 2009). Real-time PCR analysis confirmed that miR-218 was reduced in gingival fibroblasts compared with dermal fibroblasts (Figure 1).

miR-218 regulates FAK expression in fibroblasts

TGFβ synergizes with ET-1 to promote myofibroblast differentiation (Shephard et al., 2004a). Previously we found that the reduced TGFβ responsiveness observed in gingival fibroblasts compared with dermal fibroblasts could be explained by reduced endothelin-1 (ET-1) production due to decreased FAK expression and FAK/src activity in gingival fibroblasts (Guo et al., 2011a). Moreover, gingival fibroblasts are less adherent to ECM than dermal fibroblasts (Guo et al., 2011b). To assess whether miR-218 modulated FAK and ET-1 production in fibroblasts, we introduced the miR-218 precursor pre–miR-218 into gingival fibroblasts. In addition, we introduced anti–miR-218 into dermal fibroblasts. Real-time PCR analysis of RNAs prepared from gingival and dermal fibroblasts 48 h posttransfection indicated that ET-1 and FAK mRNAs were sensitive to miR-218 (Figure 2A). Moreover, transfection of the miR-218 precursor pre–miR-218 into gingival fibroblasts elevated FAK and ET-1 protein production in this cell type (Figure 2B). In addition, genome-wide expression profiling of RNA isolated from gingival fibroblasts 48 h posttransfection with the miR-218 precursor pre–miR-218 revealed that a series of profibrotic mRNAs was up-regulated in the presence of pre–miR-218, including α-SMA and CCN2 (Table 2). The expression of mature miR-218, α-SMA, and CCN2 (Leask, 2013) was verified by real-time PCR (Figure 2A). Finally, transfection of the miR-218 precursor pre–miR-218 into gingival fibroblasts promoted the adhesive ability of this cell type (Figure 3). Collectively these results suggest that miR-218 controls the adhesive ability of fibroblasts.

miR-218 regulates TGFβ activity in fibroblasts

To extend these data and provide a link between these observations, we transfected gingival fibroblasts with pre–miR-218. For RNA

Affymetrix ID	miRNA	RefSeq	Fold up-regulated, HDFs vs. HGFs
7976806	MIR136	NR_029699	2.6105
8079165	MIR138-1	NR_029700	1.70398
8109157	MIR143	NR_029684	1.96644
8109159	MIR145	NR_029686	22.1957
7976850	MIR154	NR_029704	1.81056
8068022	MIR155	NR_030784	2.08332
8157800	MIR181A2	NR_029611	1.71064
7923173	MIR181B1	NR_029612	3.71318
7916984	MIR186	NR_029707	1.86843
8008885	MIR21	NR_029493	2.50076
8094340	MIR218-1	NR_029631	12.8934
8172266	MIR221	NR_029635	3.33848
8172268	MIR222	NR_029636	3.90433
8175683	MIR224	NR_029638	3.53014
7976830	MIR299	NR_029841	1.84823
8142975	MIR29A	NR_029503	2.37767
8160439	MIR31	NR_029505	4.24258
8163107	MIR32	NR_029506	2.96918
7976832	MIR323	NR_029890	2.02766
7976842	MIR382	NR_029874	2.14901
7976848	MIR453	NR_029969	2.32701
7957608	MIR492	NR_030171	1.79965
7969574	MIR622	NR_030754	7.58325
8087881	MIRLET7G	NR_029660	2.83576

TABLE 1: microRNAs up-regulated in human dermal fibroblasts (>1.7-fold) compared to human gingival fibroblasts.
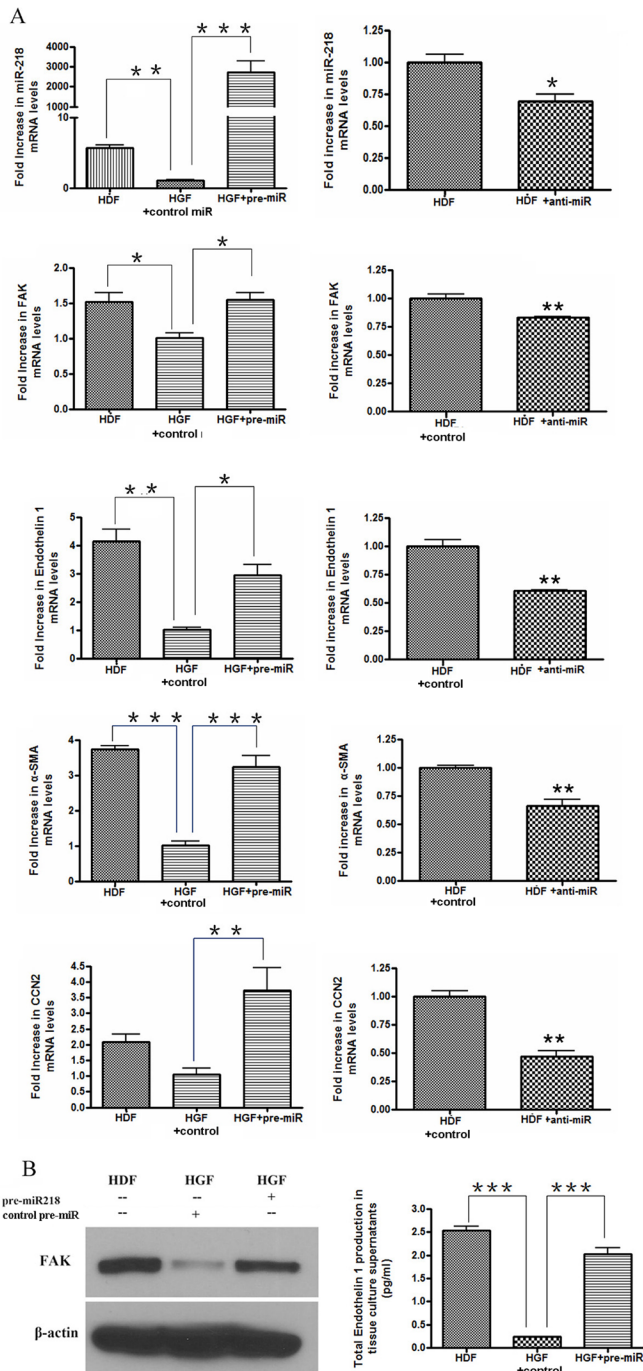
FIGURE 2: miR-218 modulates profibrotic gene expression in dermal and gingival fibroblasts. As described in *Materials and Methods*, HDFs and HGFs were transfected with anti–miR-218 or anti-miRNA negative control and pre–miR-218 or pre-miRNA negative control, respectively. Forty-eight hours posttransfection, RNA was harvested and subjected to real-time PCR analysis to detect (A) miR-218, FAK, endothelin-1, α-SMA, and CCN2 mRNAs. Average relative expression compared with HGFs ± SD ($N = 3$, *$p < 0.05$, **$p < 0.01$, ***$p < 0.001$, one-way ANOVA test). (B) Protein was assessed by Western blot analysis to detect anti-FAK and anti–β-actin antibodies or enzyme-linked immunosorbent assay (ELISA) to detect ET-1.

analysis, cells were treated with or without TGFβ1 for an additional 6 h. For protein analysis, cells were treated with or without TGFβ1 for an additional 24 h. The ability of pre–miR-218 to restore the ability of TGFβ1 to induce α-SMA mRNA and protein was shown by real-time PCR and Western blot analysis, respectively (Figure 4, A and B). Furthermore, this ability was blocked in the presence of the ALK5 inhibitor SB431542, the FAK/src inhibitor PP2, or the endothelin receptor antagonist PD145065 (Figure 4C). Conversely, the ability of TGFβ to induce ET-1 mRNA was increased in the presence of pre–miR-218 but was sensitive only to SB431542 and PP2 (Figure 4D). These results are consistent with the notion that miR-218 controls the ability of TGFβ to induce α-SMA expression via the FAK/src-dependent induction of ET-1.

Cezanne is overexpressed in gingival fibroblasts, regulates FAK and TGFβ-induced α-SMA in fibroblasts, and is a direct target of miR-218

Diminished FAK expression and activity is a feature of gingival fibroblasts (Guo *et al.*, 2011a,b). Previously it was shown that the proinflammatory transcription factor NF-κB is a key transcriptional regulator of FAK (Cox *et al.*, 2006; Ko *et al.*, 2010, 2013). NF-κB activity is very tightly regulated by endogenous cellular negative signaling regulators; for example, cezanne, a newly identified member of the A20 family of deubiquitinases, was shown to act as a negative feedback regulator of the NF-κB pathway under physiological conditions (Enesa *et al.*, 2008; Evans *et al.*, 2001). To assess whether alterations in cezanne expression might explain the reduced expression of FAK in gingival fibroblasts, we first used Western blot analysis to show that cezanne was overexpressed in gingival fibroblasts compared with dermal fibroblasts (Figure 5A). To assess whether the production of FAK in gingival fibroblasts depended on cezanne, we transfected small interfering RNA (siRNA) into gingival fibroblasts. Western blot analysis confirmed that the siRNA target cezanne could decease the expression of cezanne in gingival fibroblasts (Figure 5A). Introduction of siRNA recognizing cezanne into gingival fibroblasts caused an increase in both FAK (Figure 5, A and B) and endothelin 1 (Figure 5C) mRNA and protein expression. Similarly, the cezanne siRNA rescued the ability of gingival fibroblasts to respond to TGFβ by inducing α-SMA mRNA (Figure 5D).

TargetScan and DIANA identified two miR-218 recognition sequences between 398 and 426 and between 1414 and 1442 in the 3′ untranslated region (UTR) of cezanne (Figure 6A). The sequences 398–426 and 1414–1442 were then subcloned into pMIR-REPORT vectors and cotransfected into gingival fibroblasts with pGL4.74 in the presence or absence of pre–miR-218. The addition of prex-miR-218 reduced the luciferase activity of both pmiR-cezanne 398–426 and pmiR-cezanne 1414–1442 (Figure 6A). Mutation of these sites blocked the ability of pre–miR-218 to reduce luciferase activity (Figure 6A). In addition, real-time PCR confirmed the expression change of cezanne after overexpression or inhibition of miR-218 (Figure 6B). Western blot analysis also confirmed the change of cezanne protein level after pre–miR-218 transfection (Figure 6C). Thus pre–miR-218 targets two separate regions of the cezanne 3′ UTR. These data are consistent with the notion that miR-218 regulates TGFβ signaling by regulating cezanne/FAK. Figure 7 is a schematic diagram illustrating our findings.

DISCUSSION

Unlike skin, oral gingivae do not scar (Schor *et al.*, 1996). Instead, fibrotic responses within oral tissue are characterized by hyperproliferation and the relative absence of highly contractile myofibroblasts (Sakamoto *et al.*, 2002; Martelli *et al.*, 2010; Damasceno *et al.*, 2012). Consistent with these observations, we previously showed that, in contrast to results previously obtained using dermal fibroblasts (Kessler *et al.*, 2001), neither mechanical stress nor TGFβ potently

Affymetrix ID	RefSeq	Gene name	Fold up-regulated, pre-miR218 vs. control
		Cell adhesion	
7936968	NM_003474	ADAM metallopeptidase domain 12	1.8241
7969438	NM_005358	LIM domain 7	1.54555
8148435	NM_003882	WNT1 inducible signaling pathway protein 1	2.19884
7962579	NM_001143668	Adhesion molecule with immunoglobulin-like domain 2	3.16115
7918064	NM_001854	Collagen, type XI, α1	1.60543
8148070	NM_021110	Collagen, type XIV, α1	1.61149
8129562	NM_001901	Connective tissue growth factor	2.21101
7902687	NM_001554	Cysteine-rich, angiogenic inducer, 61	1.9717
8112971	NM_001884	Hyaluronan and proteoglycan link protein 1	1.97773
7989985	NM_001004439	Integrin, α11	1.76727
7977854	NM_032876	Jub, ajuba homologue (*Xenopus laevis*)	1.87499
8162388	NM_005014	Osteomodulin	2.01788
7961142	NM_002543	Oxidized low-density lipoprotein (lectin-like) receptor 1	1.72096
8040473	NM_004040	Ras homologue gene family, member B	1.67505
7903358	NM_001078	Vascular cell adhesion molecule 1	1.75193
		Cytoskeleton	
7934906	NM_001141945	Actin, α2, smooth muscle, aorta	2.6501
7987315	NM_005159	Actin, α, cardiac muscle 1	1.63043
8042788	NM_001615	Actin, γ2, smooth muscle, enteric	2.85741
8136347	NM_033138	Caldesmon 1	1.51663
8013015	NM_181716	Centromere protein V	1.68434
8109843	NM_004946	Dedicator of cytokinesis 2	1.51402
8098263	NM_001166108	Palladin, cytoskeletal-associated protein	1.52893
7984079	NM_000366	Tropomyosin 1 (α)	2.12499
8108873	NM_015071	Rho GTPase–activating protein 26	1.83145
8136347	NM_033138	Caldesmon 1	1.51663
8116780	NM_004415	Desmoplakin	1.58565
8047926	NM_002374	Microtubule-associated protein 2	1.60628
8169249	NM_012216	Midline 2	1.63874
8095834	NM_020859	Shroom family member 3	1.53651
7984079	NM_000366	Tropomyosin 1 (α)	2.12499

TABLE 2: Cluster analysis of mRNAs (out of 228 total) up-regulated in human gingival fibroblasts after pre–miR-218 transfection.
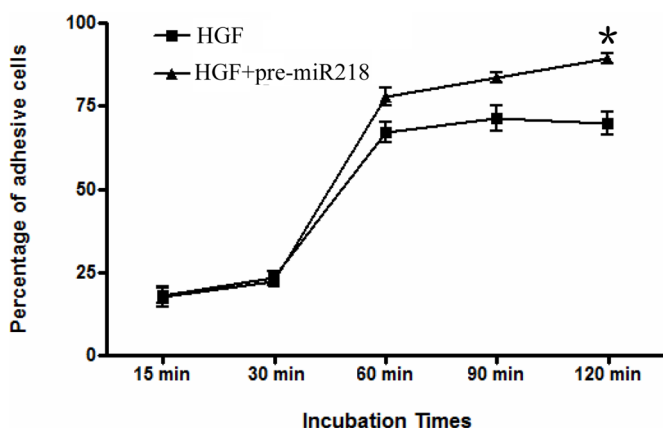
induced α-SMA expression in gingival fibroblasts (Guo *et al.*, 2011a). This difference was due to diminished basal ET-1 production caused by reduced FAK/src activity in gingival fibroblasts (Guo *et al.*, 2011a,b). Indeed, elevated adhesive signaling observed in dermal fibroblasts compared with gingival fibroblasts appeared to be crucial for the differences in TGFβ responses between the two cell types.

FIGURE 3: Transfection of pre–miR-218 into human gingival fibroblasts results in increased cell adhesion to fibronectin. As described in *Materials and Methods*, HGFs were transfected with pre–miR-218 or pre-miRNA negative control and subjected to a cell adhesion assay on fibronectin. Adherent cells were detected using MTT assay. Average ± SD ($N = 3$, *$p < 0.05$, Student's *t* test).
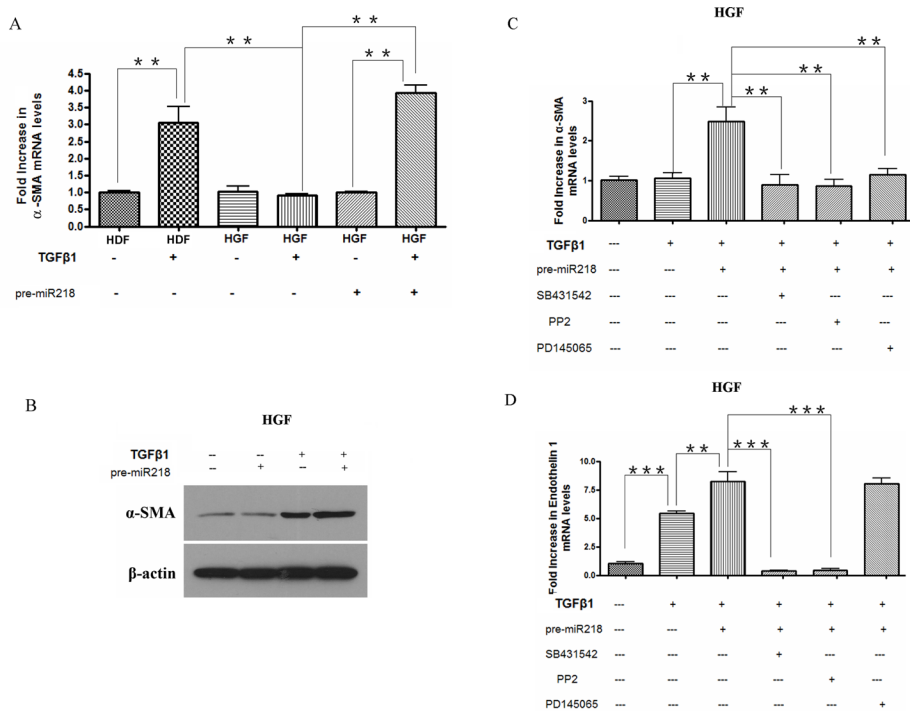
In this article, we show that miR-218 is decreased in gingival fibroblasts and ultimately responsible for the differential TGFβ responses observed in gingival versus dermal fibroblasts. Intriguingly, miR-218 was recently shown to be down-regulated post-differentiation of dental stem cells (Gay et al., 2014) and to suppress proliferation of cancer cells (Hidaka et al., 2012). To our knowledge, the concept that cezanne plays a role in TGFβ responses or fibrosis has not previously been reported. It is also interesting to note that miR-486 also regulates cezanne (Song et al., 2013).

We believe that these data are important for suggesting that the fundamental basis of scarless tissue repair could be due to epigenetic changes such as altered miR-218 expression leading to the reduced adhesive potential production of gingival fibroblasts and hence to altered TGFβ signaling. Modulating miR-218/cezanne or adhesive signaling might be useful in controlling scarring in response to injury.

MATERIALS AND METHODS
Cell culture

Gingival fibroblasts from three different human donors, identical to those previously described, were used (Thompson et al., 2010; Guo et al., 2011a,b). Each experiment using gingival fibroblasts was conducted with cells isolated from all three individuals. Human dermal fibroblasts were purchased (American Type Culture Collection, Manassas, VA). Experiments were performed on cells between passages 5 and 7. Cells were cultured in DMEM supplemented with 10% fetal bovine serum

FIGURE 4: miR-218 enhances TGFβ responses in gingival fibroblasts. (A) miR-218 promotes TGFβ-induced α-SMA expression in HGFs: RNA analysis. HGFs were treated with or without pre-miRNA negative control or pre-miR218 miRNA and treated with or without TGFβ1 for 6 h. Simultaneously, HDFs were treated with or without TGFβ1 for 6 h. RNA was harvested and subjected to real-time PCR analysis to detect α-SMA mRNA. Average ± SD (N = 3, **p < 0.01, one-way ANOVA test). (B) miR-218 promotes TGFβ-induced α-SMA expression in HGFs: protein analysis. HGFs were treated with or without pre-miRNA negative control or pre-miR218 miRNA and treated with or without TGFβ1 for 24 h. Protein was extracted and subjected to Western blot analysis with anti–α-SMA and anti–β-actin antibodies. (C, D) Effect of the ALK5 receptor inhibitor SB431542, the FAK/src inhibitor PP2, and the ET receptor antagonist PD145065 on the ability of pre–miR-218 to enhance TGFβ responses in gingival fibroblasts. Cells were treated and transfected as in A but were pretreated for 45 min before addition of TGFβ with or without DMSO, SB431542, PP2, or PD145065, as indicated. RNA was harvested and subjected to real-time PCR analysis to detect (C) α-SMA or (D) ET-1 mRNA. Average ± SD (N = 3, **p < 0.01, ***p < 0.001, one-way ANOVA test).
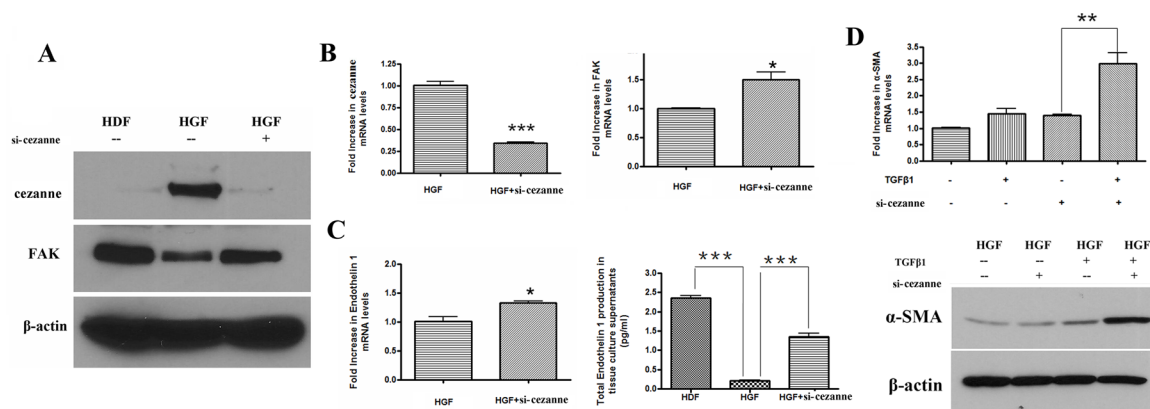

FIGURE 5: Cezanne siRNA increases FAK and TGFβ-induced α-SMA expression in gingival fibroblasts. (A) HGFs were treated with or without control siRNA or siRNA recognizing cezanne. Simultaneously, HDFs were cultured as a control. Forty-eight hours later, protein was harvested and subjected to Western blot analysis with antibodies detecting cezanne, FAK, or β-actin protein levels, Alternatively, HGFs treated as in A were subjected to (B) real-time PCR analysis to detect cezanne or FAK or (C) real-time PCR analysis or ELISA to detect ET-1 levels. (N = 3, *p < 0.05, ***p < 0.001, Student's t test). (D) Cezanne siRNA enhances TGFβ-induced α-SMA expression in HGFs. HGFs were treated with or without control siRNA or cezanne siRNA and treated with or without TGFβ1 for 6 h (for RNA analysis) or 24 h (for protein analysis). RNA was harvested and subjected to real-time PCR analysis to detect α-SMA mRNA. Average ± SD (N = 3, **p < 0.01, one-way ANOVA test). Protein was subjected to Western blot analysis to detect α-SMA or β-actin protein.
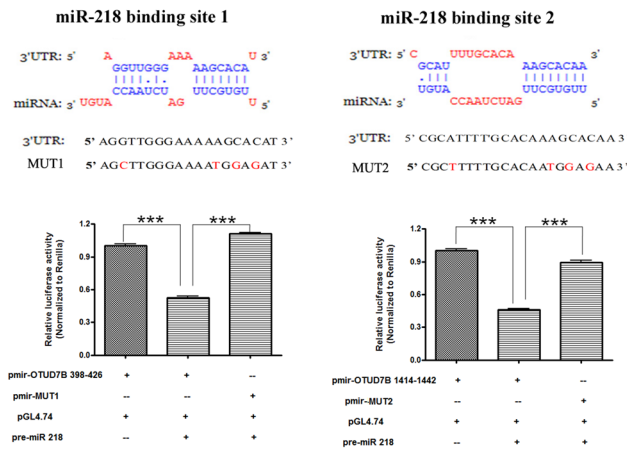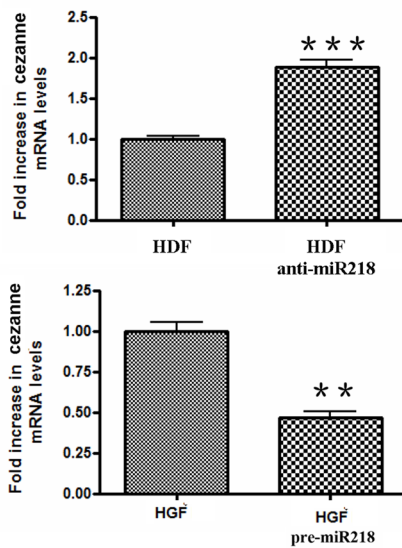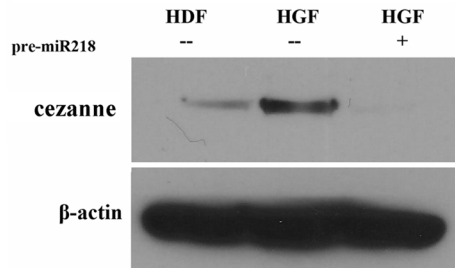
FIGURE 6: Cezanne expression is a direct target of miR-218. (A) Promoter-reporter constructs containing two predicted miR-218 recognition sequences or with the putative sequences mutated were transfected into cells with pre-miRNA negative control or pre–miR-218. Cells were cotransfected with control vector expressing *Renilla* luciferase. Adjusted average expression values ± SD ($N = 3$, **$p < 0.01$, ***$p < 0.001$, Student's *t* test). (B). HGFs were transfected with pre-miRNA negative control or pre–miR-218. In addition, HDFs were treated with anti-miRNA negative control or anti–miR-218. Forty-eight hours later, cells were harvested for RNA and subjected to real-time PCR analysis to detect cezanne ($N = 3$, **$p < 0.01$, ***$p < 0.001$, Student's *t* test). (C) HGFs were transfected with pre-miRNA negative control or pre–miR-218. As a control, HDFs were cultured in parallel. Forty-eight hours later, protein was harvested and subjected to Western blot analysis with anti-cezanne or anti–β-actin protein.

Samples were combined using One-Step Master Mix (Life Technologies), and amplified sequences were detected using the ABI Prism 7900HT Sequence Detector (Perkin Elmer Cetus, Waltham, MA) according to the manufacturer's instructions. Triplicate samples were run. Expression values were standardized to values obtained with control 18S RNA primers, using the $2^{-\Delta\Delta Ct}$ method.

Quantitative RT-PCR for mature miRNA

miR-218 expression in gingival and dermal fibroblasts was evaluated using TaqMan microRNA Assay (Applied Biosystems, Foster City, CA) as specified in the manufacturer's protocol. Real-time PCR was performed using Taqman Universal PCR master mix and ABI Prism 7900HT Sequence Detector. All reactions were performed in triplicate. Expression levels of mature microRNAs were evaluated using the $2^{-\Delta\Delta Ct}$ method.

Transfection assays

Pre–miR-218 and pre-miRNA negative control, anti–miR-218, and anti-miRNA negative control were purchased from Ambion, Burlington, Canada. SMARTpool ON-TARGET cezanne siRNA (si-cezanne) and negative control were purchased from Thermo Scientific, Ottawa, Canada. For all the assays based on miR-218 overexpression, gingival fibroblasts were cultured in DMEM/10% FBS and then transfected using siPORT NeoFX transfection agent (Invitrogen) with pre-miRNA or negative control at a final concentration of 10 nM. Cells were used for further treatment 48 h after transfection. For all the assays based on the inhibition of miR-218 expression, human dermal fibroblasts were transfected with anti-miRNA or negative control with the same method. For all the assays based on the inhibition of cezanne expression, human gingival fibroblasts were transfected with si-cezanne or negative control with the same method.

Enzyme-linked immunosorbent assays

Secreted ET-1 levels were determined in triplicate using a Quantiglo Human Endothelin-1 Immunoassay (R&D Systems, Minneapolis, MN). We used 100-μl culture supernatants in the Quantiglo immunoassay, which was performed according to the manufacturer's instructions. A standard curve (linear between 0.34 and 250 pg/ml ET-1) was conducted for each assay.

Western blotting

Protein samples (100 μg/lane) were subjected to SDS–PAGE and then transferred to polyvinylidene difluoride membranes (Invitrogen). The resultant membranes were blocked with

(FBS) and 1% antibiotic-antimycotic (Invitrogen, Burlington, ON, Canada) at 5% CO_2 and 37°C. For all experiments at least three biological replicated were used, as indicated.

Real-time PCR

Real-time PCR was performed as previously described (Thompson *et al.*, 2010; Guo *et al.*, 2011a,b). Total RNA was isolated (TRIzol; Life Technologies, Burlington, Canada) and then was reverse transcribed and amplified using TaqMan Assay-on-Demand (Life Technologies) in a 15-μl reaction volume containing two unlabeled primers and a 6-FAM–labeled TaqMan minor groove binder.
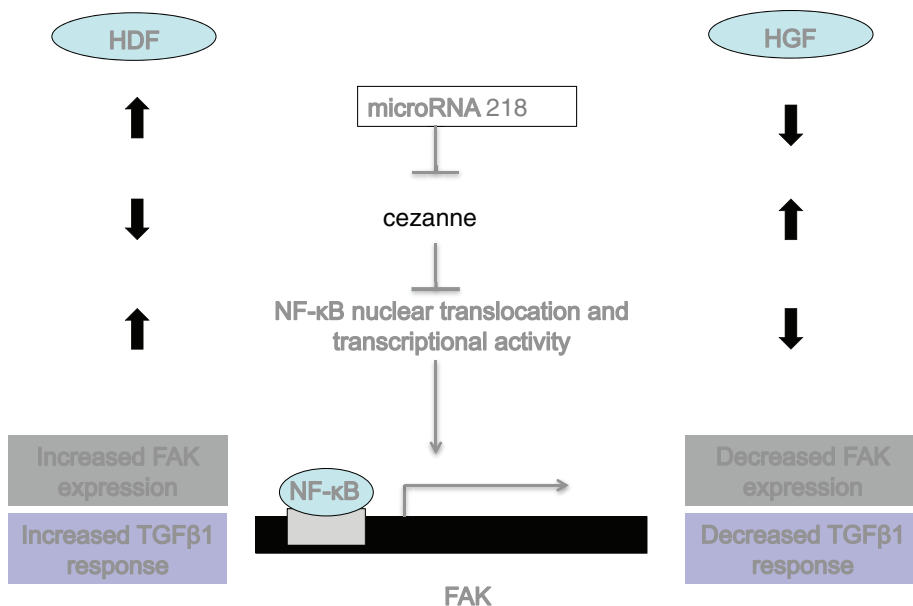
FIGURE 7: Summary of the findings. Compared to HGFs, in HDFs there is elevated miR-218 expression. miR-218 suppresses the deubiquitinase cezanne, leading to elevated FAK expression. Thus HDFs show elevated FAK-dependent transcriptional responses to TGFβ1 compared with HGF.

5% milk–Tris-buffered saline/Tween 20 (TBST) for 1 h at room temperature and then incubated with anti-FAK (Cell Signaling), anti-cezanne (Abcam), anti-CCN2 (Santa Cruz), and anti–α-SMA antibody (Sigma) overnight at 4°C, washed with TBST, incubated with appropriate secondary antibody (1:5000; Jackson Immuno-Research) conjugated to horseradish peroxidase, washed, and visualized with ECL Western Blotting Detection Reagents (Amersham Biosciences). After stripping with Restore Western Blot Stripping Buffer (Pierce) for 20 min at room temperature, membranes were processed similarly with β-actin antibody (1:10,000 dilution, Sigma-Aldrich, St. Louis, MO) as a loading control.

Expression profiling
Expression profiling was conducted essentially as previously described (Thompson et al., 2010; Guo et al., 2011a) at the London Regional Genomics Centre (Robarts Research Institute, London, Canada; www.lrgc.ca). RNA quality was assessed (Agilent Technologies, Palo Alto, CA). Single-stranded complementary DNA was prepared from 200 ng of total RNA as per the Ambion WT Expression Kit for Affymetrix GeneChip Whole Transcript WT Expression Arrays (www.ambion.com/techlib/prot/fm_4411973.pdf; Applied Biosystems, Carlsbad, CA) and the Affymetrix GeneChip WT Terminal Labeling kit and Hybridization User Manual (http://media.affymetrix.com/support/Downloads/manuals/wt_term_label_ambion_user_manual.pdf; Affymetrix, Santa Clara, CA). Total RNA was converted to cDNA and then in vitro transcribed to make cRNA. Single-stranded cDNA, 5.5 µg, was synthesized, end labeled, and hybridized for 16 h at 45°C to Human Gene 1.0 ST arrays. All liquid-handling steps were performed by a GeneChip Fluidics Station 450, and GeneChips were scanned with the GeneChip Scanner 3000 7G (Affymetrix) using Command Console, version 1.1. Probe-level (.CEL file) data were generated using Affymetrix Command Console, version 1.1. Probes were summarized to gene-level data in Partek Genomics Suite, version 6.5 (Partek, St. Louis, MO) using the RMA algorithm. Partek was used to determine gene-level analysis of variance (ANOVA) p values, fold changes, and Gene Ontology enrichment using a chi-squared test. Gene lists were then made based on fold change and p-value filters.

Adhesion assays
Cell adhesion assays were performed essentially as previously described (Guo et al., 2011b). Wells of 96-well plates were incubated overnight at 4°C with 1 µg/ml fibronectin (Sigma-Aldrich) in phosphate-buffered saline (PBS). Wells were blocked for 1 h in 1% BSA in PBS at room temperature. Gingival fibroblasts cells transfected with pre–miR-218 or negative control were harvested using 2 mM EDTA in PBS (20 min at room temperature) and then washed twice with serum-free DMEM containing 1% BSA (Sigma-Aldrich). Cells were then resuspended in the same medium (2.5×10^5 cells/ml), and 100 µl of suspension was then placed into each well for the times indicated to allow cells to attach to matrix. Nonadherent cells were removed by washing with PBS. Adherent cells were quantified by incubation with 10 µl of 3-(4,5-dimethylthiazol-2-yl)-2,5-diphenyl tetrazolium bromide (MTT) solution for 4 h at 37°C, after which formazan reaction products in each well were dissolved in 100 µl of dimethyl sulfoxide (DMSO) and A_{570} was measured. Comparison of adhesive abilities was performed by using Student's unpaired t test. A $p < 0.05$ was considered as statistically significant.

Target in vitro luciferase report assay
The pMIR-REPORT plasmids for miR-218 target cezanne 3'-UTR were constructed as pmiR-cezanne 398–426 and pmiR-cezanne 1414–1442 containing the miR-218 response element from cezanne 3'-UTR. The sequences used to create the pmiR-cezanne 398–426 are as follows: forward, 5'-CTAGTGCTCAGCAGGTTGG-GAAAAAGCACATA-3'; reverse, 5'-AGCTTATGTGCTTTTTCCCA-ACCTGCTGAGCA-3'. The sequences used to create the pmiR-cezanne 1414–1442 are as follows: forward, 5'-CTAGTGCTCAGC-CGCATT TTGCACAAAGCACAAA-3'; reverse, 5'-AGCTTTTGT-GCTTTGAGCAA AATGCGGCTGAGCA. The oligonucleotides were annealed and inserted into the pMIR-REPORT vector (Ambion). When indicated, point mutations were introduced into putative recognition sequences (Figure 6A). HEK-293 cells were plated at 55% confluency in 24-well plates and then transfected with 150 ng of the reporter plasmids, 50 ng of pGL4.74 vector, and, where applicable, 20 pmol of pre–miR-218 or control using Lipofectamine 2000 per the manufacturer's instructions (Invitrogen). Luciferase activity was measured 48 h after transfection using the Dual Luciferase Reporter Assay System (Promega, Madison, WI). Firefly luciferase activity was normalized to Renilla luciferase activity for each transfected well. Each experiment was repeated at least three times.

REFERENCES

Canady J, Karrer S, Fleck M, Bosserhoff AK (2013). Fibrosing connective tissue disorders of the skin: molecular similarities and distinctions. J Dermatol Sci 70, 151–158.

Chang HY, Chi JT, Dudoit S, Bondre C, van de Rijn M, Botstein D, Brown PO (2002). Diversity, topographic differentiation, and positional memory in human fibroblasts. Proc Natl Acad Sci USA 99, 12877–12882.

Cox BD, Natarajan M, Stettner MR, Gladson CL (2006). New concepts regarding focal adhesion kinase promotion of cell migration and proliferation. J Cell Biochem 99, 35–52.

Damasceno LS, Gonçalves Fda S, Costa e Silva E, Zenóbio EG, Souza PE, Horta MC (2012). Stromal myofibroblasts in focal reactive overgrowths of the gingiva. Braz Oral Res 26, 373–377.

Enesa K, Zakkar M, Chaudhury H, Luong le A, Rawlinson L, Mason JC, Haskard DO, Dean JL, Evans PC (2008). NF-κB suppression by the deubiquitinating enzyme Cezanne: a novel negative feedback loop in pro-inflammatory signaling. J Biol Chem 283, 7036–7045.

Evans PC, Taylor ER, Coadwell J, Heyninck K, Beyaert R, Kilshaw PJ (2001). Isolation and characterization of two novel A20-like proteins. Biochem J 357, 617–623.

Gay I, Cavender A, Peto D, Sun Z, Speer A, Cao H, Amendt BA (2014). Differentiation of human dental stem cells reveals a role for microRNA-218. J Periodontal Res 49, 110–120.

Ghosh AK, Bhattacharyya S, Lakos G, Chen SJ, Mori Y, Varga J (2004). Disruption of transforming growth factor beta signaling and profibrotic responses in normal skin fibroblasts by peroxisome proliferator-activated receptor gamma. Arthritis Rheum 50, 1305–1318.

Guo F, Carter DE, Leask A (2011a). Mechanical tension increases CCN2/CTGF expression and proliferation in gingival fibroblasts via a TGFβ-dependent mechanism. PLoS One 6, e19756.

Guo F, Carter DE, Mukhopadhyay A, Leask A (2011b). Gingival fibroblasts display reduced adhesion and spreading on extracellular matrix: a possible basis for scarless tissue repair? PLoS One 6, e27097.

Hidaka H, Seki N, Yoshino H, Yamasaki T, Yamada Y, Nohata N, Fuse M, Nakagawa M, Enokida H (2012). Tumor suppressive microRNA-1285 regulates novel molecular targets: aberrant expression and functional significance in renal cell carcinoma. Oncotarget 3, 44–57.

Kessler D, Dethlefsen S, Haase I, Plomann M, Hirche F, Krieg T, Eckes B (2001). Fibroblasts in mechanically stressed collagen lattices assume a "synthetic" phenotype. J Biol Chem 276, 36575–36585.

Ko BS, Chang TC, Liou JY (2010). Focal adhesion kinase as a therapeutic target of bortezomib. Anticancer Agents Med Chem 10, 747–752.

Ko BS, Jan YJ, Chang TC, Liang SM, Chen SC, Liu TA, Wu YM, Wang J, Liou JY (2013). Upregulation of focal adhesion kinase by 14-3-3ε via NFκB activation in hepatocellular carcinoma. Anticancer Agents Med Chem 13, 555–562.

Leask A (2013). CCN2: a novel, specific and valid target for anti-fibrotic drug intervention. Expert Opin Ther Targets 17, 1067–1071.

Li X, Shen Y, Ichikawa H, Antes T, Goldberg GS (2009). Regulation of miRNA expression by Src and contact normalization: effects on nonanchored cell growth and migration. Oncogene 28, 4272–4283.

Liu S, Xu SW, Kennedy L, Pala D, Chen Y, Eastwood M, Carter DE, Black CM, Abraham DJ, Leask A (2007). FAK is required for TGFbeta-induced JNK phosphorylation in fibroblasts: implications for acquisition of a matrix-remodeling phenotype. Mol Biol Cell 18, 2169–2178.

Mann J, Mann DA (2013). Epigenetic regulation of wound healing and fibrosis. Curr Opin Rheumatol 25, 101–107.

Martelli H Jr, Santos SM, Guimarães AL, Ṕaranaíba LM, Laranjeira AL, Coletta RD, Bonan PR (2010). Idiopathic gingival fibromatosis: description of two cases. Minerva Stomatol 59, 143–148.

Mishra R, Zhu L, Eckert RL, Simonson MS (2007). TGF-beta-regulated collagen type I accumulation: role of Src-based signals. Am J Physiol Cell Physiol 292, C1361–C1369.

Sakamoto R, Nitta T, Kamikawa Y, Kono S, Kamikawa Y, Sugihara K, Tsuyama S, Murata F (2002). Histochemical, immunohistochemical, and ultrastructural studies of gingival fibromatosis: a case report. Med Electron Microsc 35, 248–254.

Schor SL, Ellis I, Irwin CR, Banyard J, Seneviratne K, Dolman C, Gilbert AD, Chisholm DM (1996). Subpopulations of fetal-like gingival fibroblasts: characterisation and potential significance for wound healing and the progression of periodontal disease. Oral Dis 2, 155–166.

Shephard P, Hinz B, Smola-Hess S, Meister JJ, Krieg T, Smola H (2004a). Dissecting the roles of endothelin, TGF-beta and GM-CSF on myofibroblast differentiation by keratinocytes. Thromb Haemost 92, 262–274.

Shephard P, Martin G, Smola-Hess S, Brunner G, Krieg T, Smola H (2004b). Myofibroblast differentiation is induced in keratinocyte-fibroblast co-cultures and is antagonistically regulated by endogenous transforming growth factor-beta and interleukin-1. Am J Pathol 164, 2055–2066.

Song L et al. (2013). miR-486 sustains NF-κB activity by disrupting multiple NF-κB-negative feedback loops. Cell Res 23, 274–289.

Thannickal VJ, Lee DY, White ES, Cui Z, Larios JM, Chacon R, Horowitz JC, Day RM, Thomas PE (2003). Myofibroblast differentiation by transforming growth factor-beta1 is dependent on cell adhesion and integrin signaling via focal adhesion kinase. J Biol Chem 278, 12384–12389.

Thompson K, Hamilton DW, Leask A (2010). ALK5 inhibition blocks TGFβ-induced CCN2 expression in gingival fibroblasts. J Dent Res 89, 1450–1454.

Wynn TA, Ramalingam TR (2012). Mechanisms of fibrosis: therapeutic translation for fibrotic disease. Nat Med 18, 1028–1040.